HAL open science

Impact of overflow vs. limitation of propionic acid on poly(3-hydroxybutyrate-co-3-hydroxyvalerate) biosynthesis

Coline Perdrier, Estelle Doineau, Ludivine Leroyer, Maeva Subileau, Helene Angellier-Coussy, Laurence Preziosi-Belloy, Estelle Grousseau

To cite this version:

Coline Perdrier, Estelle Doineau, Ludivine Leroyer, Maeva Subileau, Helene Angellier-Coussy, et al.. Impact of overflow vs. limitation of propionic acid on poly(3-hydroxybutyrate-co-3-hydroxyvalerate) biosynthesis. Process Biochemistry, 2023, 128, pp.147-157. 10.1016/j.procbio.2023.02.006 . hal-04002228

HAL Id: hal-04002228

https://hal.inrae.fr/hal-04002228

Submitted on 18 Oct 2023

HAL is a multi-disciplinary open access archive for the deposit and dissemination of scientific research documents, whether they are published or not. The documents may come from teaching and research institutions in France or abroad, or from public or private research centers.

L'archive ouverte pluridisciplinaire **HAL**, est destinée au dépôt et à la diffusion de documents scientifiques de niveau recherche, publiés ou non, émanant des établissements d'enseignement et de recherche français ou étrangers, des laboratoires publics ou privés.

Distributed under a Creative Commons Attribution - NonCommercial - NoDerivatives 4.0 International License

Impact of overflow vs. limitation of propionic acid on poly(3-hydroxybutyrate-*co*-3-hydroxyvalerate) biosynthesis

Published in Process Biochemistry, Volume 128, May 2023, Pages 147-157, https://doi.org/10.1016/j.procbio.2023.02.006

Coline Perdrier, Estelle Doineau, Ludivine Leroyer, Maëva Subileau, Hélène Angellier-Coussy, Laurence Preziosi-Belloy, Estelle Grousseau*

UMR IATE, Univ Montpellier, INRAE, Institut Agro, Montpellier, France

coline.perdrier@umontpellier.fr, estelle.doineau@umontpellier.fr, leroyer-ludivine@outlook.com, maeva.subileau@supagro.fr, helene.coussy@umontpellier.fr, laurence.preziosi-belloy@umontpellier.fr, estelle.grousseau@umontpellier.fr

* UMR IATE, Univ Montpellier, INRAE, Institut Agro, Place Eugène Bataillon, CC23, Bat. 15, 3ème étage, 34095 Montpellier Cedex 5, FRANCE ; estelle.grousseau@umontpellier.fr ; +33(0)4 67 14 33 53

Graphical Abstract

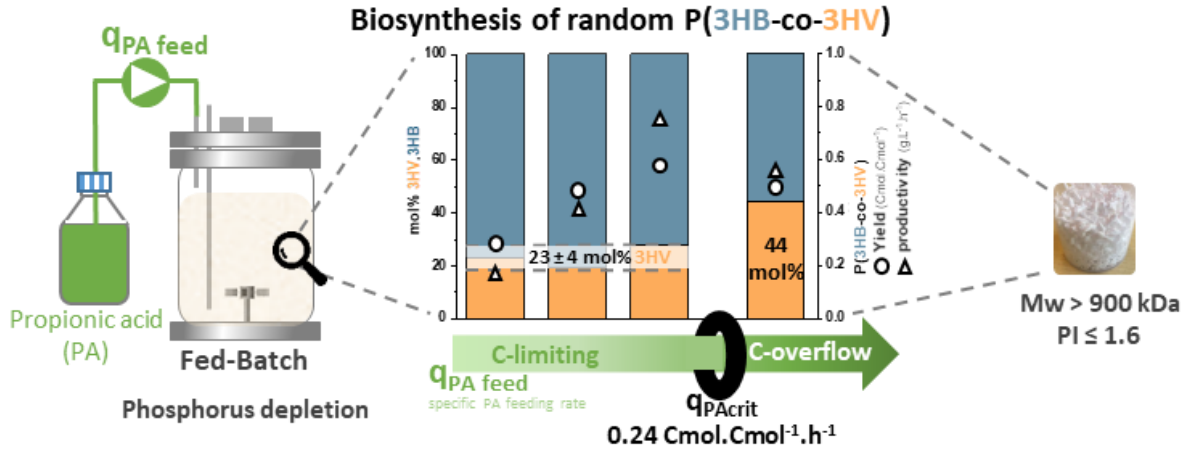

Abstract

The 3HV content of poly(3-hydroxybutyrate-co-3-hydroxyvalerate) (P(3HB-co-3HV)), a biobased and biodegradable polyester, must be controlled for improved thermomechanical properties. Propionic acid (PA) is the main acid allowing 3HV monomer biosynthesis which is present in volatile fatty acid mixes produced from agro-industrial coproducts acidogenesis. With the strain *Cupriavidus necator,* we investigated the impact of carbon-limiting vs. carbon-overflow conditions thanks to fed-batch cultures, with sequential or continuous feeding of propionic acid as the sole carbon source, and phosphorus deficiency conditions. Regardless of the C-limiting continuous specific feeding rate imposed (i.e., below the determined critical specific feeding rate (q_{PAcrit}) of 0.24 Cmol.Cmol^{-1}.h^{-1}), a regular incorporation of the 3HV in the copolymer at a content of 23 ± 4 mol% was observed with a high molecular weight

(≈ 1000 kDa) and a remarkably low polydispersity index (≈ 1.5). This feeding strategy maximized both the productivity (up to 0.78 $g.L^{-1}.h^{-1}$) and conversion yield of propionic acid into P(3HB-co-3HV) (up to 0.59 $Cmol.Cmol^{-1}$) if operated close to q_{PAcrit}. With C-overflow sequential feeding (i.e., above q_{PAcrit}), the residual propionic acid concentration has been highlighted as a key parameter in 3HV content improvement (≥ 44 mol%) even though it occurred at the expense of the copolymer yield and productivity.

Keywords

Cupriavidus necator; phosphorus deficiency; specific feeding rate; propionic acid accumulation; 3HV content; structural and melting characteristics

1 Introduction

Polyhydroxyalkanoates (PHAs) are linear polyesters produced by various microorganisms as intracellular carbon and energy storage materials. Among them, the homopolymer polyhydroxybutyrate (P(3HB)) was the first to be studied and marketed [1]. Since then, The copolymer poly(3-hydroxybutyrate-co-3-hydroxyvalerate) P(3HB-co-3HV) has gained much attention because the increasing incorporation of comonomers of 3-hydroxyvalerate (3HV) from at least 8 mol% up to 45-50 mol% can improve PHA-based material flexibility and increase the thermal processing window by decreasing both crystallinity, melting temperature and glass transition temperature, thus allowing for expansion of possible areas of applications [2–4].

The biosynthesis of PHAs occurs generally when microorganisms are exposed to unbalanced growth conditions and is modulated depending on which essential nutrients, such as nitrogen (N) and phosphorus (P), or electron acceptors, such as oxygen (O_2), are limiting [1,5–7]. Although nitrogen limitation is most commonly used, phosphorus limitation has been proven to be effective. Indeed, P deficiency can lead to a higher synthesis of PHAs [8–10] and a polymer richer in 3HV than that obtained under nitrogen limitation conditions [11]. *C. necator* (formerly *Ralstonia eutropha*) is widely known as a model PHA-producing bacterium that can use a broad range of substrates, such as sugars, organic acids and C1 gases [5,12]. It is typically used as pure culture for the production of PHAs at a large scale as it is known to accumulate up to 80-90 wt% of its own mass and to biosynthesize the P(3HB-co-3HV) copolymer [5,12]. With this strain, 3HV biosynthesis requires precursor compounds structurally related to 3HV, i.e., odd carbon-numbered substrates such as propionic or valeric acid [13,14]. The proportion of 3HV in the copolymer is usually controlled by the percentage of these odd carbon-numbered substrates among other available carbon sources in the feed [11,15–18]. For example, increasing the proportion of propionic acid in a mixture with butyric acid from 25 mol% to 100 mol% led to an increase in the proportion of 3HV in the copolymer from 4 to 32 mol% [11], and a maximum of 50 to 56 mol% 3HV was reached with propionic acid as the sole carbon and energy source [11,17].

Propionic and valeric acids are usually found in mixes of volatile fatty acids (VFAs) obtained from anaerobic digestion of agro-industrial coproducts [3,19,20]. The use of so-called waste streams in a biorefinery approach would reduce both the environmental impact and the cost of PHA production [1,20–23], thus allowing higher market penetration. Much effort has been made to manipulate the composition of VFA mixtures by means of fermentation conditions [20,24]. However, the percentage of VFA with an odd number of carbon obtained depends on the agro-industrial residues used, their intrinsic variability and the fermentation process used [25–30]. It would therefore be interesting to

control the 3HV content by adapting the feeding strategy according to the percentage and concentration of odd-numbered acids in the volatile fatty acid mixture. Even if the fraction of valeric acid in VFA mixes can exceptionally reach 26 or 35 wt% (COD basis) after fermentation of waste activated sludge or sugar cane molasses [25,26], valeric acid is usually nonexistent [27–29] or in low proportion (4 to 15 wt%) [26,29,30] after acidogenesis of various coproducts. In contrast, propionic acid is systematically present [25–30] in the range of 10 to 25 wt% and up to 30 to 39 wt% (COD basis), as reported by [25,28,30]. To investigate the impact of feeding strategies of VFA mixtures on 3HV percentage during P(3HB-co-3HV) biosynthesis, propionic acid therefore constitutes a more relevant model of odd carbon-numbered substrate. Up to now, different feeding strategies have been studied: pulse-wise additions [3,6,7,31–33], constant feeding [34,35] or a supply based on biological demand such as pH-stat feeding (i.e., propionic acid is fed automatically to maintain the pH of the culture broth at a constant value [33,36–38]), or a combination of pH-and-DO-stat feeding [39] where dissolved oxygen (DO) is used as carbon exhaustion indicator. Nevertheless, the impact of the feeding mode on HV percentage has been scarcely documented, and the intensity of the feeding rate (i.e., carbon metabolic flux) as part of the feeding strategy has not been investigated as a potential tool to tailor copolymer biosynthesis with respect to carbon limiting (C-limiting) vs. carbon overflow (C-overflow) conditions.

The objective of the present work was to investigate the impact of the intensity of the feeding rate on the biosynthesis performances of the model strain *C. necator* (especially yields and productivity) and on the structural and melting properties of the recovered copolymers. P(3HB-co-3HV) production was triggered by phosphorus deficiency and conducted in fed-batch mode using propionic acid as the unique carbon and energy source. An exploratory experiment (FB1) was performed to determine the threshold in terms of the specific propionic acid feeding rate (q_{PAfeed}) between C-limiting conditions and C-overflow conditions beyond which a flux fraction cannot be assimilated by cells and accumulates in the broth. Then to study the impact of several stabilized specific feeding rates (q_{Pafeed}) of continuously provided propionic acid, experiments (FB2 and FB3) were performed below $q_{Pacrit,}$ (i.e., under C-limiting conditions). These C-limiting conditions were compared with C-overflow conditions experienced in cultivation of FB1 by providing propionic acid with a q_{PAfeed} over the critical threshold. Before the P(3HB-co-3HV) production phase in fed-batch mode, the biomass production phase with glucose as the carbon and energy source must be mastered and reproducible (kinetically and stoichiometrically) to be able to perform the comparison work mentioned above.

2 Materials & Methods

2.1 Strain and growth conditions

The strain *C. necator* DSM 545 (or H1 $G^{+}3$) was purchased from DSMZ (Germany). DSM 545 is a spontaneous mutant of the strain DSM 529 (H1) and is able to catabolize glucose, unlike the wild-type *C. necator* DSM 428 (H16). *C. necator* cells were preserved as frozen stock in liquid tryptic soy broth (TSB – Sigma Aldrich) with 20% (v/v) glycerol at -80 °C.

Frozen stock was streaked on TSA plates (TSB with addition of 20 $g.L^{-1}$ agar). The plate was incubated for 24–48 h at 30 °C. From a single colony, three successive precultures were prepared in Erlenmeyer flasks containing chemically defined (CD) medium with a level of inoculation of 5% (v/v) under aerobic conditions in an orbital shaker (160 rpm, Fisher Bioblock Scientific) at 30 °C and a pH of 7. The third preculture was grown for 30 h and used to inoculate the bioreactor. The CD medium contained (per

liter) 5 g glucose as the carbon source, 1 g NH_4Cl as the nitrogen source, 9 g $Na_2HPO_4 \cdot 12H_2O$, 1.5 g KH_2PO_4, 0.2 g $MgSO_4 \cdot 7H_2O$, 4.5 mg $FeSO_4 \cdot 7H_2O$, 4 mg $CaCl_2$ and 0.1% (v/v) trace element solution. The stock trace element solution had the following composition (per liter): 2.4 g H_3BO_3, 1.6 g $CoCl_2 \cdot 6H_2O$, 0.44 g $ZnSO_4 \cdot 7H_2O$, 3 g $MnSO_4 \cdot 7H_2O$, 0.3 g $CuSO_4 \cdot 5H_2O$, 0.25 g $Na_2MoO_4 \cdot 2H_2O$ and 0.16 g $NiCl_2 \cdot 6H_2O$.

2.2 Biomass production and P(3HB-co-3HV) synthesis in the bioreactor

All cultures were prepared in a 30-liter instrumented fermentor (INFORS, working volume of 20 L). with an initial volume of 16 L and an initial biomass concentration of approximately 0.1 $g.L^{-1}$. The temperature was controlled at 30 °C, and the pH was controlled at 7 (InPro 3030/200, Mettler Toledo, Switzerland) by the addition of NH_4OH solution. Dissolved oxygen (DO) was measured with an Ingold polarographic probe and maintained at or above 35% air saturation by adjusting the inlet air flow rate and the agitation up to 800 rpm. A biomass optical probe with a broadband NIR (Model 653/BT65, Wedgewood, USA) and conductivity probe (BIOMASS system, Fogale Nanotech, France) were immersed in the broth. Both CO_2 and O_2 outlet gases were measured online using a gas analyzer (Abiss LC 312, Mocon-Dansensor, France). Foam formation was avoided by automatic addition of a 10% (v/v) anti-foam aqueous solution (Biospumex 153 K, PMC Ouvrie, France). The added masses of carbon source (i.e., propionic acid, NH_4OH and anti-foam solutions were monitored in a real time course by weight recording. Data acquisition and online monitoring were handled by the homemade software BossView implemented using LabVIEW 6.1 (National Instruments, USA).

The CD medium composition for biomass production in the bioreactor was slightly modified: (i) the concentration of glucose was increased to 20 $g.L^{-1}$ (and not higher to avoid significant inhibition by glucose [9,10]), targeting 8 to 10 $g.L^{-1}$ of biomass according to the growth yields reported in the literature (0.4 to 0.5 $g_{Xt}.g_{Glc}^{-1}$ [6,40,41]); (ii) the total phosphorus concentration was designed to provide only the quantity of P sufficient to form 8 $g_{Xr}.L^{-1}$ of biomass (using the biomass production yield of 55 $g_{Xr}.g_P^{-1}$ [42]) and was hence decreased to 140 $mg.L^{-1}$ (supplied by 0.6 $g.L^{-1}$ $Na_2HPO_4 \cdot 12H_2O$ and 0.1 $g.L^{-1}$ KH_2PO_4 in addition to phosphorus left in the inoculum); (iii) K_2SO_4, 1.9 $g.L^{-1}$ was added to compensate for the decrease in K linked to the change in KH_2PO_4 concentration; and (iv) the $(NH_4)_2SO_4$ concentration was decreased to 1.3 $g.L^{-1}$ as pH maintenance was ensured by the addition of NH_4OH solution (9.5-9.8 M). In addition, during the batch step, 8 $mg.L^{-1}$ $CaCl_2$, 9 $mg.L^{-1}$ $FeSO_4 \cdot 7H_2O$ and 0.44 $mg.L^{-1}$ $ZnSO_4 \cdot 7H_2O$ were added to the broth.

The biomass production steps in batch mode using glucose as the carbon and energy source were followed by in situ fed-batch polymer production steps using a concentrated propionic acid solution as the sole carbon source (400 $g.L^{-1}$) at different specific feeding rates (q_{PAfeed}). Fed-batch cultivations were stopped after the uptake of 1.0 to 1.2 kg of propionic acid, ensuring a similar amount of propionic acid assimilated, i.e., a similar progress level of the reaction.

2.3 Analytical procedures

2.3.1 Total biomass and its elemental composition

Total biomass (Xt), expressed in $g.L^{-1}$, was monitored online with the optical density (OD) probe and was calibrated against the biomass dry weight. The biomass dry weight was determined gravimetrically after drying the washed sample to a constant mass at 105 °C. Optical density was also quantified off-line with a spectrophotometer (PRIM, SECOMAM, France) in a 1 cm optical path cuvette at 620 nm (OD_{620}) after appropriate dilutions with a saline solution (8 $g.L^{-1}$ NaCl) and was calibrated against biomass dry weight. The elemental composition of biomass of *C. necator* was quantified by CHNS/O

analysis using a Vario Micro Cube and thermal conductivity detection, which were performed by the 'Laboratoire de Mesures Physiques', analytical facilities of Montpellier University, from washed and freeze-dried biomass. Phosphorus measurements were performed by inductively coupled plasma-optical emission spectroscopy (ICP–OES iCap 7400 Duo) by the 'AETE-ISO, OSU-OREME laboratory', analytical facilities of Montpellier University.

2.3.2 Monomeric composition of P(3HB-co-3HV)

The monomeric composition of P(3HB-co-3HV) was determined by an acid butanolysis method adapted from [43,44] and gas chromatography (GC-FID). For this purpose, butanolysis was performed by resuspending 20 mg of the preground washed and freeze-dried biomass samples or calibration standards (methyl-hydroxybutyrate (Sigma–Aldrich) and methyl-hydroxyvalerate (Sigma–Aldrich)) in 2 mL of a solution of butanol acidified with concentrated HCl (75:25, w:w) containing 0.5 $g.L^{-1}$ methyl-hexanoate (Sigma–Aldrich). The sealed tubes were incubated at 100 °C for 3 h with vortex mixing for 10 s every hour and then cooled in an ice water bath for 5 min. The ester derivatives were then extracted by adding 2.5 mL of hexane and 4 mL of ultrapure water, vortex mixing (10 s) and then incubating (10 min) in an ice water bath for phase separation. The underlying aqueous phase was removed, and the extraction step was repeated by adding 4 mL of ultrapure water. The recovered organic phase was centrifuged (10 min, 2500 rcf) to remove any solid debris, dried with Na_2SO_4, transferred directly to standard 2 mL GC vials and stored at -20 °C prior to analysis. The butyl esters were analyzed by a Shimadzu GC 2010 Plus gas chromatograph equipped with a flame ionization detector and an AOC20I automatic sampler (injected volume: 0.2 µL). The capillary column was an Agilent DB-5HT column (15 m x 0.25 mm x 0.1 µm film thickness). The helium carrier flow pressure was controlled at 37.5 kPa, and the split ratio was 25:1. The temperature conditions were as follows: injector 280 °C; detector 400 °C; and oven 60 to 70 °C at 2 °C min^{-1}, then to 120 °C, at 5 °C.min^{-1}, and finally to 390 °C, at 35 °C.min^{-1}, with a 5 min hold time.

2.3.3 Glucose, propionic acid and phosphorus analysis

The supernatants obtained after sample centrifugation were filtered through a 0.2 µm membrane prior to analysis. The concentrations of glucose (Glc) and propionic acid (PA) were measured by HPLC (Shimadzu, Japan) equipped with an Aminex HPX-87H column (300 x 7.8 mm, Biorad, USA) operated at 50 °C and with 5 mM H_2SO_4 as the mobile phase at 0.5 mL.min^{-1} and using RI and UV–VIS at 210 nm detectors (Shimadzu RID-10A and SPD-20A, Kyoto, Japan). The detection limit was 0.5 $g.L^{-1}$ and 0.1 $g.L^{-1}$ for glucose and propionic acid, respectively. The residual phosphorus measurements in supernatants were performed as described in the section *Total biomass and its elemental composition*.

2.4 Calculations

2.4.1 PHA content and residual biomass (Xr)

The PHA content was calculated as the percentage of the ratio of the PHA (P(3HB) or P(3HB-co-3HV)) concentration to the total biomass concentration.

$$PHA\ content\ (wt\%) = \frac{\mathrm{PHAs}}{Xt}.100 \quad (1)$$

The residual biomass (Xr) concentration was calculated by subtracting the P(3HB-co-3HV) contribution from the total amount of biomass (i.e., Xt).

$$Xr = Xt - PHAs \quad (2)$$

2.4.2 Broth volume calculation

The evolution of the culture broth volume was calculated accounting for the volume of the aqueous phase (including the initial volume and water addition from feeding solutions) (Vaq), the volume of wet suspended cells (Vsc) and the volume of sampling (Vsp):

$$V = Vaq + Vsc - Vsp \quad (3)$$

where $Vsc = Xt \times V/(\sigma \times \rho)$ (4) [45,46], σ is the dry matter fraction, and ρ is the density of the microorganism (see Supplementary material S1 for calculation details and $\sigma.\rho$ term estimation).

$$V = (Vaq - Vsp)/(1 - \frac{Xt}{\sigma.\rho}) \quad (5)$$

2.4.3 Productivity, yields, specific rates and carbon balance

All calculations were performed on consumed and produced amounts of substrates or products. This means that the amounts present in the reactor (concentrations multiplied by the broth volume), masses withdrawn by sampling, and any initial masses in the reactor were taken into account for both substrates and products. All amounts referring to g or Cmol equivalents of biomass were calculated using a molar mass of 25.58 ± 0.80 $g_{Xr}.Cmol^{-1}$ obtained from biomass elemental composition free from PHAs (average of 13 samples from the 3 experiments).

The overall yields of biomass production related to substrates ($Y_{Glc,Xr}$, $Y_{P,Xr}$, and $Y_{N,Xr}$) were calculated as the total Xr produced divided by the total amount of substrates consumed (Glc, P or N). The growth rates (μ) were obtained by linear regression of the logarithm of the amount of total biomass as a function of time.

For each studied period of cultivation identified in gray in the figures, the production yield of polymer ($Y_{PA,\ PHA}$) was calculated by linear regression on the relationship between the amounts of monomer units produced against the amount of propionic acid consumed. The specific feeding rate (q_{PAfeed}) or production rates of 3HB units (q_{3HB}) and 3HV units (q_{3HV}) were based on the derivative function of the amount of substrate provided or produced monomer over time divided by the mass of residual biomass. As long as no accumulation of the substrate in the medium was measured, the specific propionic acid uptake rate (q_{PA}) was equal to q_{PAfeed}. The overall carbon balance was assessed by the ratio of carbon-containing product mass (PHAs, Xr, and CO_2) to carbon consumed (Glc and PA).

2.4.4 3HV content of newly produced polymer (%HV_{NPP})

The molar percentage of 3HV of newly produced polymer (%HV_{NPP}) [38], also called %HV^{inst} in some references [11], is defined as the ratio of q_{3HV} to the cumulated specific production rates of both monomers (q_{3HB} and q_{3HV}).

$$\%HV_{NPP} = \frac{q_{3HV}}{q_{3HV}+q_{3HB}}.100 \quad (6)$$

2.4.5 Respiratory quotient (RQ)

Experimentally, RQ was calculated from O_2 consumption and CO_2 production rates determined in line with the gas analyzer and is expressed in $Mole_{CO2}.Mole_{O2}^{-1}$:

$$RQ = \left|\frac{r_{CO2}}{r_{O2}}\right| \quad (7)$$

The theoretical respiratory quotient (RQ) is given by the following general equation:

$RQ_{S,P}^{theo} = \left| \frac{\gamma_{O2}}{\gamma_S} \frac{1-Y_{S,P}}{1-\frac{\gamma_P}{\gamma_S}Y_{S,P}} \right|$ (8) where S is the substrate (Glc or PA) and P is the product formed by biological reaction (i.e., biomass, P(3HB) or P(3HB-co-3HV) (see Supplementary material S2).

2.4.6 Maintenance energy

Maintenance energy was assessed using the Herbert-Pirt equation [47]:

$q_{PA} = q_{PA \to PHA} + m$ (9) where m is the substrate fraction needed for maintenance energy and potential other non-PHA products.

Equation (9) combined with yield definitions ($Y_{PA,PHA}^{exp} = \frac{q_{PHA}}{q_{PA}}$ and $Y_{PA,PHA}^{theo} = \frac{q_{PHA}}{q_{PA \to PHA}}$) leads to the following linear relation:

$\frac{1}{Y_{PA,PHA}^{exp}} = \frac{1}{q_{PHA}} \times m + \frac{1}{Y_{PA,PHA}^{theo}}$ (10) with the theoretical yield of PHA production from propionic acid $Y_{PA,PHA}^{theo}$ set to 0.69 Cmol.Cmol^{-1} according to [11] (see Supplementary material S3).

Equation (10) was used to assess the m factor expressed in Cmol.Cmol^{-1}.h^{-1} from the experimentally determined PHA production yield $\left(Y_{PA,PHA}^{exp}\right)$ and PHA specific production rate (q_{PHA}):

2.5 P(3HB-co-3HV) characterization

2.5.1 P(3HB-co-3HV) chemical extraction

Washed and freeze-dried biomass was refluxed (4 h, 65 °C) with 50 mL chloroform per gram of biomass and vigorous magnetic stirring as reported in Burniol-Figols et al., 2018 [48]. Afterward, the latter suspension was filtered under vacuum on PVDF membranes with a 0.45 µm pore size (Merck Durapore), the retentate was rinsed with a small amount of chloroform, and the filtrate containing solubilized polymers was recovered. The resulting solvent solution was concentrated approximately 5-fold by rotary evaporation (30 °C under vacuum). P(3HB-co-3HV) was then precipitated by dropwise addition of the concentrated solution into a large amount of ice-cold absolute ethanol [49] under strong agitation (chloroform/ethanol ratio: 1:10 v/v), recovered by vacuum filtration over sintered glass (porosity of 10 to 16 µm) and then washed with ethanol. Finally, the polymer was dried at 30 °C under vacuum for 24 h and stored under controlled conditions (23 °C and 50% RH) before characterization.

2.5.2 Size exclusion chromatography (SEC)

The weight-averaged molecular weight ($\bar{M}_w$), as well as the polydispersity index (PI), were determined by the Toulouse White Biotechnology (TWB) Institute using size exclusion chromatography associated with multiangle light scattering (SEC-MALS) and refractive index detectors (both from Wyatt Technology Corp). The polymer samples were dissolved at room temperature (i.e., 20 °C) in 5 mL chloroform in HeadSpace vials with PTFE caps for 3 h under magnetic agitation. The latter solution was transferred to a 10 mL graduated flask at a concentration of approximately 2 g.L^{-1} and filtered through 0.45 µm PTFE membranes before injection in duplicate into the SEC apparatus. Monodisperse 30 kDa polystyrene, prepared under the same conditions as the samples, was used to calibrate both detectors. The refractive index increment (dn/dc) in chloroform used was 0.16 mL.g^{-1} [50] and 0.0336 mL.g^{-1} [51] for PS and P(3HB-co-3HV), respectively.

2.5.3 Differential scanning calorimetry (DSC)

Differential scanning calorimetry (DSC) tests were performed using Q200 equipment (TA Instruments, USA) with nitrogen as the purge gas (50 mL.min^{-1}). Samples of approximately 5 to 10 mg of P(3HB-co-3HV) powders were placed in sealed aluminum pans (TA Instruments, New Castle USA). The thermal cycle was a first heating from -30 °C to 180 °C, then an isotherm at 180 °C for 5 min, and then cooling to -30 °C, with heating/cooling rates of 10 °C.min^{-1}. The measurements were performed at least in duplicate.

2.5.4 Nuclear magnetic resonance (NMR) spectroscopy

Samples were dissolved (20 mg.mL^{-1}) in deuterated chloroform ($CDCl_3$) at room temperature for 30 min and filtered through 0.2 µm PTFE filters. P(3HB-co-3HV) ^{1}H and ^{13}C NMR spectra were obtained by the technical platform of Charles Gerhardt Institute of Montpellier on a Bruker spectrometer Ascend III HD operating at 400 MHz (^{1}H) and 100 MHz (^{13}C) as described by [52] with the following modifications: (i) 3.6 kHz for spectral width and 64 scans for the ^{1}H NMR spectra setup; (ii) 10 kHz for transmitter frequency offset for the ^{13}C NMR spectra. Quantitative conditions were obtained with a 30° pulse (3.3 µs) and a relaxation delay at 1 s for ^{1}H measurements and can be considered as best as possible for ^{13}C (without relaxation delay determination). ^{1}H decoupling was applied during acquisition (Waltz16 with a pulse of 90 µs). The solvent resonance peak was used as a chemical shift reference at 7.26 ppm for ^{1}H and 77 ppm for ^{13}C NMR.

The molar fractions of 3HB (F_B) and 3HV (F_V) were obtained by integrating signals from the branching end groups from ^{1}H NMR spectra with the doublet resonance at 1.26 ppm and the triplet resonance at 0.89 ppm, respectively. The sequence distribution of monomers along the P(3HB-co-3HV) chain could be assessed by (i) determining the F_{VV}, F_{BV}, F_{VB}, and F_{BB} molar fractions (where F_{XY} is the molar fraction of the XY sequence) by integrating signals of carbonyl groups from ^{13}C spectra and (ii) evaluating the extent of the deviation (*D* parameter) of the copolymer composition from the statistically random compositional distribution (i.e., Bernoullian statistic model) [53] with the following equation:

$$D = \frac{F_{VV} \times F_{BB}}{F_{VB} \times F_{BV}} \quad (11)$$

The *D* value is 1 for statistically random copolymers, greater (typically considered above 1.5 [54]) than 1 for "blocky" copolymers, or less than 1 for alternating copolymers.

3 Results & Discussion

3.1 Biomass production phase in batch mode

For the three experiments, considering initial concentrations of 19.6 ± 0.3 g.L^{-1} for glucose and 140 ± 14 mg$_P$.L^{-1} for phosphorus, the total glucose uptake led as expected to the production of 8.1 ± 0.9 g$_{Xt}$.L^{-1} of biomass and a depletion of phosphorus (P in the broth lower than 2 mg$_P$.L^{-1}) (Figure 1.A). The biomass comprised 12 ± 5 wt% P(3HB) corresponding to the core of PHA granules subsequently expanded with P(3HB-co-3HV). Similar P(3HB) contents at the end of the non-limiting growth phase from 8 to 20 wt% were obtained [6,41,55]. The production of P(3HB) induced at the end of the growth phase while P was being depleted in the medium corresponds to a metabolic change that can be monitored by the evolution of the respiratory quotient (RQ). Indeed, in the example depicted in Figure 1.B, biomass production from glucose is characterized by an average RQ of 1.05 ± 0.03 before 23.3 h of cultivation, which is consistent with a theoretical $RQ_{Glc,X}^{theo}$ of 1.11 (taking into account our experimental $Y_{Glc,Xr}$, see Supplementary material S3). At 23.3 h of cultivation, a significant increase in

RQ occurred in agreement with P(3HB) synthesis: RQ stabilized at 1.28 ± 0.02 (23.9 to 24.7 h), which corresponds to 96% of the theoretical RQ ($RQ^{theo}_{Glc,P(3HB)} = 1.34$, see Supplementary material S3). These observations also interestingly enabled us to define a phosphorus concentration threshold at 7 $mg_P.L^{-1}$, beyond which the metabolic activity of cells changed and P(3HB) synthesis was favored.

These experimental conditions allowed us to obtain a good repeatability of biomass production in terms of (i) specific growth rate (0.16 ± 0.01 h^{-1}); (ii) global yields of residual biomass from a carbon source ($Y_{Glc,Xr}$ = 0.42 ± 0.01 $g_{Xr}.g_{Glc}^{-1}$), phosphorus ($Y_{P,Xr}$ = 59 ± 5 $g_{Xr}.g_P^{-1}$) and nitrogen ($Y_{N,Xr}$ = 7.0 ± 1.1 $g_{Xr}.g_N^{-1}$); and consequently (iii) residual elemental composition ($CH_{1.94\pm0.02}O_{0.47\pm0.05}N_{0.25\pm0.00}P_{0.014\pm0.001}S_{0.005\pm0.001}$). This repeatability, i.e., constant biomass production, was a mandatory step in the study of the subsequent P(3HB-co-3HV) biosynthesis phase.

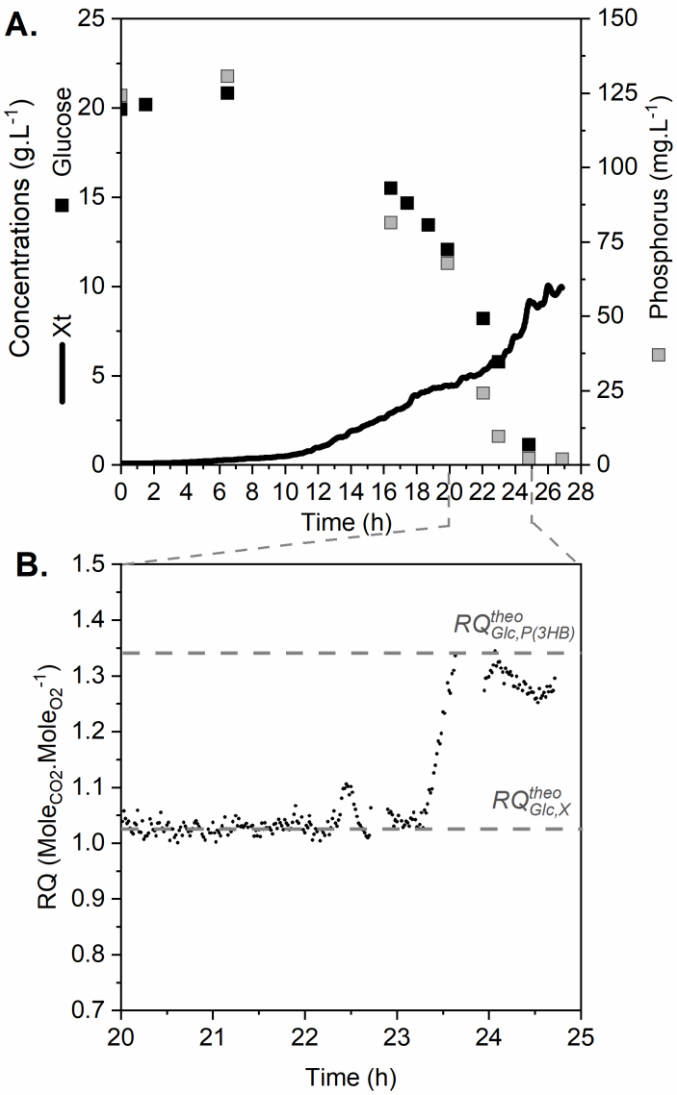

Figure 1: Example of the time course of a biomass production phase (batch preliminary to FB2 experiment) with glucose as carbon and energy source until double carbon and phosphorus depletion; (A) concentrations of residual substrates (glucose and phosphorus) and total biomass (Xt); (B) zoom of 20 to 25 hours on the measured RQ.

3.2 Determination of the critical specific uptake rate of propionic acid (q_{PAcrit}) of *C. necator*

An exploratory fed-batch (FB1) was performed to determine the critical specific uptake rate of propionic acid. The changes in specific feeding rate (q_{PAfeed}) during the fed-batch are shown in Figure 2.A. From 46 to 52 h, the feeding rate was increased stepwise from 0.17 to 0.28 $Cmol.Cmol^{-1}.h^{-1}$ with stabilized steps of at least 0.7 h (the first studied period shaded in gray in Figure 2.B and C). Online indicators (dissolved oxygen, O_2 consumption rate and CO_2 production rate) showed an increase in metabolic activity proportional to the increase in substrate provision and were stable for each feeding rate period. No propionic acid was detected in the broth during this phase (Figure 1.B), and medium conductivity was characterized by constant values (data not shown). Simultaneously, the PHA content in biomass increased from 4 wt% to approximately 20 wt% (Figure 2.C) , which confirmed the conversion of the carbon substrate into copolymer P(3HB-co-3HV), as expected. However, after 5.2 h of feeding stabilization at 0.28 $Cmol.Cmol^{-1}.h^{-1}$, an accumulation of propionic acid in the medium (2.5 $g.L^{-1}$) was measured. This accumulation occurred earlier as a decrease in metabolic activity was noticeable with the online indicators from 2.7 h after the switch (progressive decrease in O_2 consumption and in CO_2 production) and was then confirmed by an increase in medium conductivity from 3.5 h after the switch (data not shown). All of these signals actually demonstrate that the cells were not able to fully assimilate the carbon flow of 0.28 $Cmol.Cmol^{-1}.h^{-1}$, and the actual propionic acid uptake rate (q_{PA}) was estimated to be approximately 0.24 $Cmol.Cmol^{-1}.h^{-1}$. The q_{PAcrit} of the *C. necator* strain was hence determined to be approximately 0.24 $Cmol.Cmol^{-1}.h^{-1}$ under phosphorus depletion conditions.

From 56 h to 60 h (beginning of the unshaded area of Figure 2), a cessation of propionic acid feeding was performed to allow PA consumption by the cells. Then, at 60 h, different specific feeding rates were applied sequentially depending on propionic acid accumulation. The overflow of carbon was confirmed: all specific feeding rates tested at 0.24 $Cmol.Cmol^{-1}.h^{-1}$ (sequential feeding period FB1.2 in gray on Figure 2.A, period studied in Part 3.4) and up to 0.31 $Cmol.Cmol^{-1}.h^{-1}$ also led to an accumulation of the substrate (up to 5.5 $g.L^{-1}$ measured; see Figure 2.A and B).

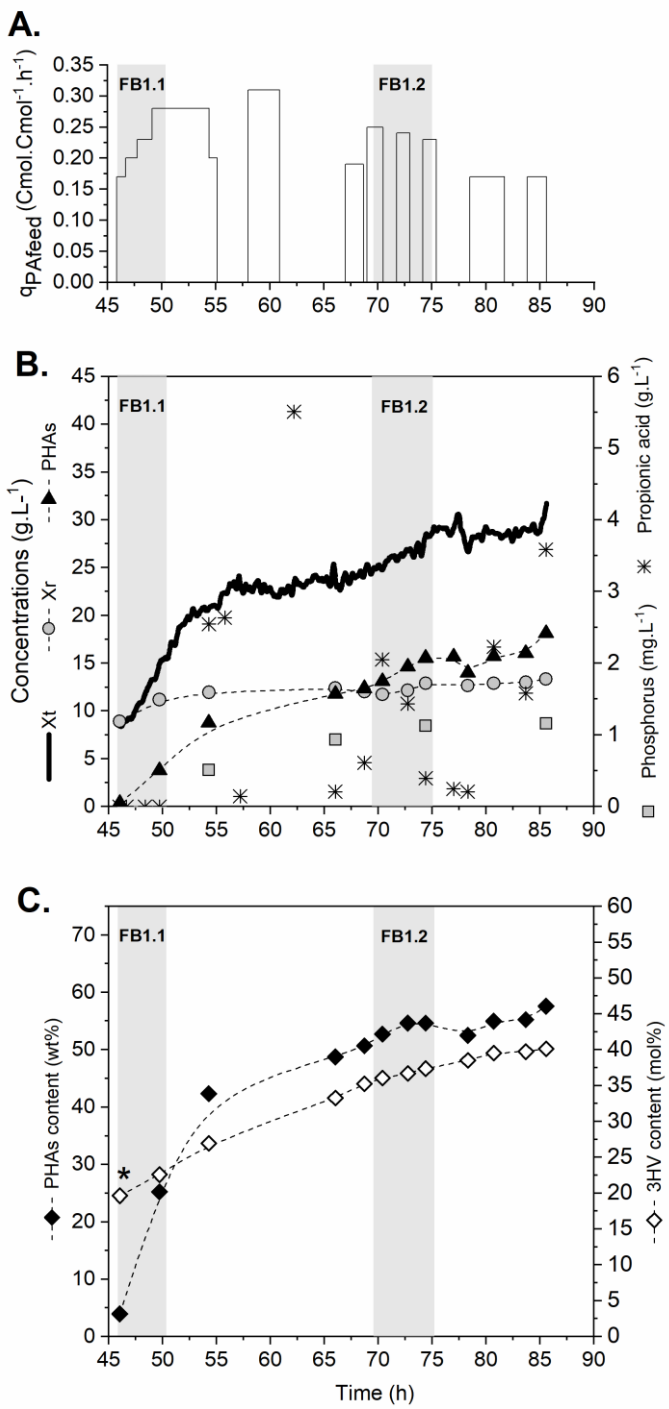

Figure 2: Time course of P(3HB-co-3HV) biosynthesis during exploratory experiment FB1 performed with stepwise increases in propionic acid feeding (45 h to 56 h) and sequential feeding (from 56 h). (A) Specific feeding rates applied (q_{PAfeed}); (B) concentrations of residual substrates (propionic acid, phosphorus) and products (total biomass (Xt), residual biomass (Xr), and PHAs); (C) PHA weight content in the biomass and 3HV molar content in the copolymer. The studied period used to calculate the kinetic and stoichiometric parameters in Table 1 is displayed as a gray shaded area * Beginning of the studied period FB1.1 is characterized by a 3HV content in the copolymer of 20 mol% as a pulse of propionic acid was used to assess the substrate uptake rate prior to fed-batch initiation (time period not displayed).

Interestingly, when the feeding rates were below the critical rate (0.17 to 0.19 $Cmol.Cmol^{-1}.h^{-1}$ at 67, 78 or 84 h) were applied, slight accumulations of propionic acid were measured (Figure 2.A and B). Is this decrease in substrate uptake rate capacity linked to the reaction progress level (phosphorus deficiency and PHA content higher than or equal to 50 wt% PHAs) and/or to repeated accumulations of propionic acid? This point must be checked under propionic acid limitation conditions.

3.3 Continuous feeding and propionic acid-limiting conditions ($q_{PAfeed} < q_{PAcrit}$) for P(3HB-co-3HV) biosynthesis

To avoid any accumulation of propionic acid in the medium and thus any influence of a parameter other than the specific feeding rate of propionic acid (q_{PAfeed}) on copolymer production, the following experiments (FB2 and FB3) were performed with a continuous q_{PAfeed} below the critical threshold previously determined to be 0.24 $Cmol.Cmol^{-1}.h^{-1}$ (Figure 3). These productions were preceded by an intermediate phase, i.e., a gradual adaptation to propionic acid as the sole source of carbon and energy by increasing the feeding rate stepwise (unshaded areas Figure 3). The feeding rate was then stabilized in the FB2 fed-batch at 0.08 $Cmol.Cmol^{-1}.h^{-1}$ during 12.4 h (Figure 3AB, FB2.1 studied period) and 0.10 $Cmol.Cmol^{-1}.h^{-1}$ for 46.3 h (Figure 3 AB, FB2.2 studied period) and in FB3 at 0.17 $Cmol.Cmol^{-1}.h^{-1}$ for 32.5 h (Figure 2CD, FB3.1 studied period). This feeding strategy worked successfully: propionic acid was not detected in the broth regardless of the rate applied (see Figure 3), meaning that the specific consumption rate of propionic acid was equal to the feeding rate (q_{PAfeed}). Interestingly, a value corresponding to 70% of the q_{PAcrit} (q_{PAfeed} of 0.17 $Cmol.Cmol^{-1}.h^{-1}$) could be maintained for 32.5 h (FB3.1) until the end of the cultivation, where cells exhibited up to 71% PHAs, while the same rate applied at 78 h and 84 h in the previous sequential feeding batch (FB1) led to propionic acid accumulation (Figure 2.A, B). This leads to the conclusion that the decrease in propionic acid assimilative capacity experienced in the FB1 exploratory experiment is not linked to the reaction progress level (phosphorus deficiency and PHA content higher than or equal to 50 wt% PHAs) but rather to repeated accumulations of propionic acid and linked stresses.

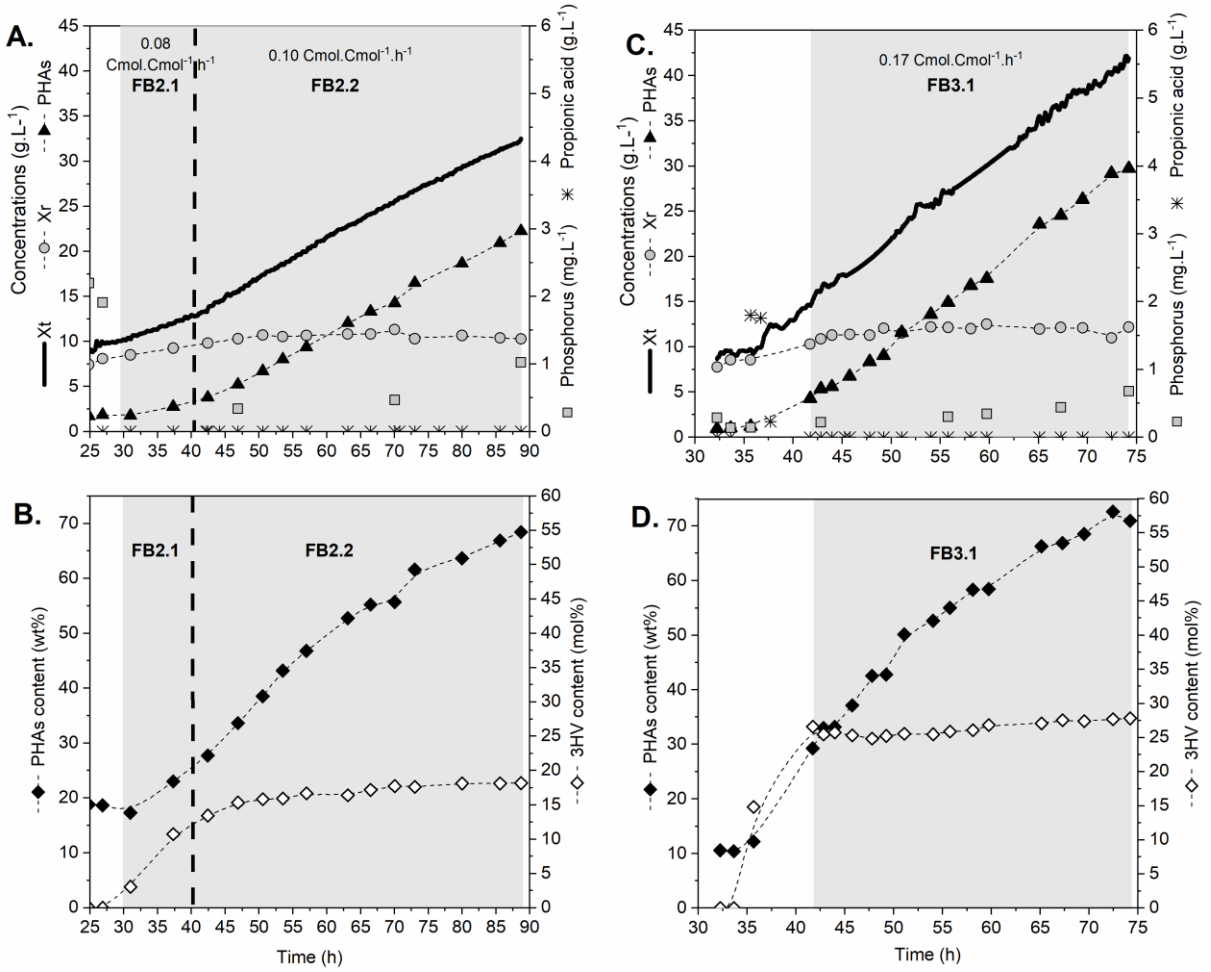

Figure 3: Time course of P(3HB-co-3HV) biosynthesis during experiments FB2 (A and B) and FB3 (C and D) performed with continuous limiting propionic acid feeding. (A, C) Concentrations of residual substrates (propionic acid, phosphorus) and products (total biomass (Xt), residual biomass (Xr), and PHAs); (B, D) PHA weight content in biomass and 3HV molar content in the copolymer. The studied period used to calculate the kinetic and stoichiometric parameters in Table 1 is displayed as a gray shaded area.

Table 1: Fed-batch P(3HB-co-3HV) biosynthesis phases studied and their main stoichiometric and kinetic characteristics

Exp.	Studied period*	Feeding strategy		Duration (h)	q_{PAfeed} (Cmol. $Cmol^{-1}.h^{-1}$)	Q_{PHA} ($g.L^{-1}.h^{-1}$)	$Y_{PA,PHA}$ (Cmol. $Cmol^{-1}$)	Carbon balance (%Cmol)	% HV_{NPP} (mol%)	RQ (Mol_{CO2}. Mol_{O2}^{-1})	q_{3HB} (Cmol. $Cmol^{-1}.h^{-1}$)	q_{3HV} (Cmol. $Cmol^{-1}.h^{-1}$)
FB2	FB2.1	PA-lim	Cont.	12.4	0.08 ± 0.00	0.17	0.28 ± 0.01	95	23	0.86 ± 0.01	0.02 ± 0.00	0.01 ± 0.00
	FB2.2	PA-lim	Cont.	46.3	0.10 ± 0.00	0.40	0.48 ± 0.00	95	19	0.86 ± 0.01	0.04 ± 0.01	0.01 ± 0.00
FB3	FB3.1	PA-lim	Cont.	32.5	0.17 ± 0.01	0.78	0.59 ± 0.00	103	28	0.87 ± 0.03	0.06 ± 0.00	0.03 ± 0.00
FB1	FB1.1	PA-lim	Step Incr.	3.3	0.17–0.23	nd	nd	nd	23	nd	nd	nd
	FB1.2	PA-overflow	Seq.	6.4	0.24 ± 0.01	0.56	0.50	nd	44	nd	0.03 ± 0.01	0.03 ± 0.01

*gray shaded area displayed in Figures 2 and 3

The volumetric productivities of PHAs (Q_{PHA}) calculated for the stabilized studied periods FB2.1, FB2.2 and FB3.1 were 0.17, 0.40 and 0.78 $g.L^{-1}.h^{-1}$, respectively (Table 1). Thus, increasing the q_{PA} under carbon-limiting conditions increases P(3HB-co-HV) productivity. This productivity depends on both the propionic acid specific uptake rate (q_{PA}), the yield of PHA production from propionic acid ($Y_{PA,PHA}$) and the residual biomass concentration (Xr):

$$Q_{PHA} = q_{PHA} \times X_r = Y_{PA,PHA} \times q_{PA} \times X_r \quad (10)$$

As Xr was similar for the studied phases, whether this increase in productivity was only related to the increase in the propionic acid specific uptake rate (q_{PA}) or whether there was a concomitant increase in production yields ($Y_{PA,\ PHA}$) was interesting to explore. As shown in **Erreur ! Source du renvoi introuvable.**, both increased twofold indeed as the specific propionic acid uptake rate increased from 0.08 to 0.17 $Cmol.Cmol^{-1}$ (**Erreur ! Source du renvoi introuvable.**). The theoretical conversion yields ($Y_{PA,PHA}^{theo}$) for the production of such a copolymer are between 0.47 $Cmol.Cmol^{-1}$ and 0.69 $Cmol.Cmol^{-1}$ depending on the ratio between the NADPH cofactor regeneration pathway used (the two extreme scenarios being the 100% tricarboxylic acid cycle pathway and 100% Entner-Doudoroff (ED) pathway as reported in [11]; see Table A2 Supplementary file S3). The experimental $Y_{PA,PHA}$ of 0.59 $Cmol.Cmol^{-1}$ obtained at 0.17 $Cmol.Cmol^{-1}.h^{-1}$ (FB3.1) suggested that the NADPH,H+ pool would be regenerated by both pathways (ED and TCA). However, for the lowest q_{PA} set (i.e., FB2.1), the experimental yield of 0.28 $Cmol.Cmol^{-1}$ is far from the theoretical value even if considering that the $NADPH/H^+$ pool would be regenerated only by the TCA pathway. As the carbon balance is over 95% complete in this phase, this result suggests a carbon spill. Indeed, even if the metabolism is severely energy-limited due to nutrient deficiency, it still addresses a carbon fraction to cell maintenance, i.e., to essential functions such as proton motive force, osmoregulation or the degradation of intracellular macromolecules. The maintenance energy m, considered constant in the classical Herbert-Pirt model used here, could be estimated from the data of the stabilized studied period FB2.1, FB2.2 and FB3.1 at 0.044 $Cmol.Cmol^{-1}.h^{-1}$ (see Supplementary file S4) and explain the decrease in yield observed with the decrease in q_{PA}. Notably, this maintenance value is consistent with the reported maintenance for PHA biosynthesis from VFAs under P limitation [56].

The overall mole fraction of 3HV in the copolymer increased significantly up to 45 hours (FB2) and 42 hours (FB3) (Figure 3. B, D) and then tended to stabilize over time to finally reach 18 and 28 mol% 3HV, respectively. For studying the impact of q_{PA} on the production kinetics of the two monomers, the respiratory quotient (RQ) was not a good indicator because it stabilized at a similar value for the 3 studied periods (0.86 ± 0.03 $Mol_{CO2}.\ Mol_{O2}^{-1}$) (**Erreur ! Source du renvoi introuvable.**) close to the theoretical value ($RQ_{PA,PHA}^{theo}$ = 0.84–0.85 $Mol_{CO2}.Mol_{O2}^{-1}$, see Supplementary materials S3). Thus, a relevant parameter was necessary and should not take into account the history of granule formation (such as the core of P(3HB) produced during the biomass production phase). This is the 3HV content in the newly produced polymer ($\%HV_{NPP}$), which was calculated using the specific production rates of polymer (q_{PHA}), 3HB (q_{3HB}) and 3HV (q_{3HV}) throughout the carbon-limiting period (FB2.1, FB2.2 and FB3.1). Those specific rates were found to be constant, resulting in a steady incorporation of 3HV into P(3HB-co-3HB) and thus a constant $\%HV_{NPP}$ of 23, 19 and 28 mol% for specific feeding rates of 0.08, 0.10 and 0.17 $Cmol.Cmol^{-1}.h^{-1}$, respectively (**Erreur ! Source du renvoi introuvable.**). These relatively close values do not seem to be directly related to the specific feeding rate. Under conditions of propionic acid limitation, a similar value (23 mol% HV_{NPP}) could be calculated during the exploratory fed-batch, where the feeding rate was gradually increased from 0.17 to 0.23 $Cmol.Cmol^{-1}.h^{-1}$ without

accumulation of propionic acid in the culture broth (FB1.1 in Figure 2 and Table 1). Thus, regardless of the imposed rate (tested range: 0.08 to 0.23 $Cmol.Cmol^{-1}.h^{-1}$) below the critical specific uptake rate q_{PAcrit} under propionic acid limiting conditions, no impact was found on the 3HV molar fraction in the polymer characterized by an average value of 23 ± 4%.

Interestingly, the structural characteristics of the copolymers extracted with chloroform at the end of the reaction do not appear to be influenced by the intensity of the feeding under propionic acid-limiting conditions. Polymers with high molecular weight ($\overline{M}w$) between 900 and 1100 kDa were collected with a fairly narrow chain size distribution, and the polydispersity index (PI) was below 1.7 (Table 2) allowing to assume good thermo-mechanical properties [57]. The 3HV content in the extracted copolymer was calculated from the 1H-NMR spectra and found to be identical to that calculated from the GC analysis (Table 2) and consistent with the 3HV fraction measured in the copolymer inside the cells (Figure 2C and 3BD). 13C-NMR data was used to calculate the nearest neighbour statistics *D* value and determine the PHA microstructure. This parameter is used to evaluate the extent of the deviation of the copolymer from the statistically random distribution of the composition (i.e., the Bernoulli model). For all copolymers, a value very close to 1 is measured (1.1 and 0.9), showing that independent of the specific propionic acid feed rate, the copolymer is characterized by a random monomer distribution (Table 2) in accordance with the kinetics of the biosynthesis characterized by a regular incorporation of 3HV monomers.

Table 2: Molecular structure and melting behavior of P(3HB-co-3HV) copolymers of different molar fractions of 3HV recovered from experiments FB1, FB2 and FB3

Exp.	Molecular structure						Melting behavior	
	3HV molar content (%)		D from ^{13}C NMR	$\overline{M}w$ (kDa)	PI	P(3HB) core (wt%)	$T_{m.1}$ (°C)	$T_{m.2}$ (°C)
	Chemically determined	Determined from ^{1}H NMR*						
FB2	17	18	1.10	901 ± 0	1.42 ± 0.00	7.5	133.0 ± 1.1	159.5 ± 0.1
FB3	28	28	0.94	1112 ± 27	1.61 ± 0.02	3.0	101.6 ± 0.1	160.1 ± 0.5
FB1	40	40	1.06	1055 ± 54	1.59 ± 0.01	1.5-3.3	76.0 ± 0.4	162.3 ± 0.3

*Only data obtained from ^{1}H resonance measurements are presented as data processing from ^{13}C spectra resulted in the same 3HB/3HV ratio in the copolymers

3.4 Propionic acid overflow versus limitation conditions

As the 3HV content in the newly produced polymer was limited to 23 ± 4% HV_{NPP} when the specific propionic acid feed rate (q_{PAfeed}) was lower than the critical flow rate (q_{PAcrit}), a q_{PAfeed} equal to or higher than the q_{PAcrit} was applied to assess the impact of the propionic acid overflow on the 3HV proportion but also on the biosynthesis performance, such as yields or productivities, as well as on the characteristics of the polymer produced. For this purpose, the sequential feeding period (FB1.2 in Figure 2) was compared with the continuous feeding periods and, in particular, to the one with the highest stabilized q_{PAfeed}, 0.17 $Cmol.Cmol^{-1}.h^{-1}$ (FB3.1 in Figure 3). During the sequential feeding period FB1.2, the q_{PAfeed} value was set to 0.24 ± 0.01 $Cmol.Cmol^{-1}.h^{-1}$ during 1.4 h, 1.2 h and 1.2 h with feeding interruption in between these periods (Figure 2.A). The end of the feeding interruption was determined by the sudden increase in dissolved O_2 linked with propionic acid exhaustion in the broth. As expected, this feeding condition resulted in an accumulation of propionic acid in the medium between 0.4 and 2.1 $g.L^{-1}$ (Figure 2.B). However, the most interesting result is the 3HV content in the newly produced polymer, which reached 44 mol% (Table 1), a value twice as high as the average value obtained under carbon limitation conditions (23 ± 4% HV_{NPP}). As shown in Table 1, this increase in

$\%HV_{NPP}$ is not explained by a significant increase in q_{3HV} but by a decrease in q_{3HB} from 0.06 to 0.03 $Cmol.Cmol^{-1}.h^{-1}$, while q_{3HV} is maintained at 0.03 $Cmol.Cmol^{-1}.h^{-1}$. A previous study under similar conditions mainly attributed this phenomenon to severe phosphorus limitation [11,58], but our results clearly show that independent of phosphorus deficiency, the decline in 3HB biosynthesis seems to be essentially due to overflow of propionic acid, which results in its accumulation in the culture medium. Indeed, for the same amount of propionic acid assimilated (between 1050-1190 g) in P deficiency, propionic acid accumulation conditions (FB1.2) allow a decrease in the instantaneous supply of HB, which leads to an enrichment of the polymer in HV (Table 1).

To our knowledge, the impact of the residual propionic acid concentration on the 3HV content has not been demonstrated thus far; even when revisiting previously published studies, some evidence of it can be found. In batch culture, the increase in the initial concentration of propionic acid generates an increase in the HV content [59]. Other work using propionic acid as a cosubstrate with glucose (fed-batch cultivation at a ratio of 0.52 $mol_{PA}.mol_{Glc}^{-1}$) also observed continuous propionic acid accumulation in the medium up to 7.5 $g.L^{-1}$ together with a continuous increase in the 3HV content [16].

However, if residual PA has a positive impact on HV content, it has a negative impact on yields and productivity: a global $Y_{PA,\,PHA}$ of 0.50 $Cmol.Cmol^{-1}$ could be calculated for sequential feeding phase FB1.2 against 0.59 $Cmol.Cmol^{-1}$ for the continuous feeding period FB3.1, and productivity decreased by a factor of 1.4, while the specific propionic acid feeding rate was approximately 1.4 times higher (**Erreur ! Source du renvoi introuvable.**).

As a result of this sequential feeding strategy with residual PA in the broth during the FB1 experiment, the final copolymer comprised 40 mol% 3HV (Figure 2C and Table 2). The copolymer has a molecular weight ($\overline{M}w$) of 1055 ± 54, a polydispersity index (PI) of 1.59 ± 0.01 and a *D* parameter value of 1.06 corresponding to that of a random copolymer such as the one obtained with continuous feeding in propionic acid limiting conditions (Table 2). Other authors screening different strategies (cofeeding and alternate feeding with variable periods) to feed propionate and butyrate did not observe significant variations in $\overline{M}w$ [3]. Thus, despite the various specific propionic acid feeding rates tested (below and above q_{PAcrit}) throughout this experiment leading to periods without or with residual PA in the broth, the polymer could not be defined as a blocky polymer based on the NMR results. On the DSC thermogram (Figure 4), when heating the copolymer from -20 °C to 180 °C, two well-separated endothermic peaks were observed. The low-melting temperature fraction ($T_{m,1}$), corresponding to the main contribution to the melting enthalpy, was attributed to the produced random copolymer rich in high HV units. $T_{m,1}$ decreased with increasing 3HV content, from 133 °C for 18 mol% 3HV to 76 °C for 40 mol% 3HV (Figure 4, Table 2). Nevertheless, the melting behavior of the polymer FB1 shows a broader main endothermic peak than those observed from the FB2 and FB3 profiles with an irregular profile (multihumped), suggesting the coexistence of crystals with different sizes and/or types. This observation could be the consequence of the various feeding rates tested throughout the experiment FB1, which resulted in different carbon distributions, i.e., the coexistence of copolymer fractions with different 3HV contents. The high-melting temperature fraction ($T_{m,2}$) equaled 160-162 °C for all copolymers independent of the 3HV content (Figure 4, Table 3) and was attributed to polymer chains with very low 3HV content, or even P(3HB), and may correspond to the melting of the granule core comprising P(3HB) which can account for up to 7.5 wt% of the copolymer (**Erreur ! Source du renvoi introuvable.**2). This granule core was due to the transition from cell growth on glucose to P(3HB-co-

3HV) production on propionic acid (see Part 3.1). Fully or partially melting those P(3HB) crystals when using thermal processes is a key point in the subsequent crystallization behavior that could be interesting depending on targeted properties. To understand and study the impact of this P(3HB) core, it would be necessary to produce the same polymers without the P(3HB) core. To do this, it is necessary to adjust the phosphorus or glucose requirements in the initial culture medium such that the cells consume the P(3HB) produced before starting the biosynthesis phase of P(3HB-co-3HV) on propionic acid only. Indeed, phosphorus would have to be depleted after the depletion of glucose. The respiratory quotient (RQ) could then be used again to check the metabolic shift toward PHB consumption as biomass production from P(3HB) should be characterized by an RQ of approximately 0.85-0.89 (see supplementary material S2) against an RQ of approximately 1.05 for growth on glucose or approximately 1.28 for P(3HB) production on glucose.

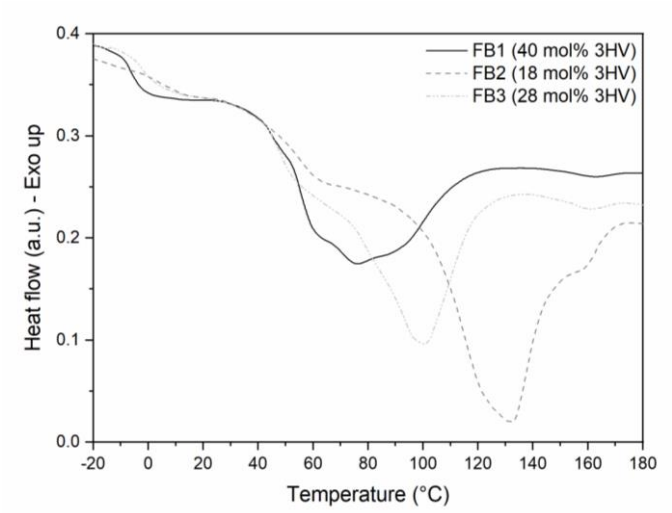

Figure 4: DSC thermograms (first heating ramp) of P(3HB-co-3HV) copolymers recovered from exploratory experiment FB1 combining propionic acid limiting conditions and propionic acid overflow conditions (solid line) or from the FB2 and FB3 experiments performed with continuous feeding under propionic acid-limiting conditions only (dashed lines).

4 Conclusion

The threshold in terms of the specific propionic acid feeding rate (q_{PAfeed}) between C-limiting conditions and C-overflow conditions, when *C. necator* cells are subjected to P depletion to trigger P(3HB-co-3HV) biosynthesis, has been determined at 0.24 $Cmol.Cmol^{-1}.h^{-1}$ (q_{PAcrit}). This preliminary step allowed us to study C-limiting vs. C-overflow conditions on biosynthesis performances (especially yields and productivity, which are of major importance in reducing the cost of PHA production) and on the structure and melting properties of the recovered copolymers essential to predicting their processing behavior and properties.

Regardless of the specific continuous feeding rate imposed in C-limiting conditions (i.e., below the critical specific feeding rate), a regular incorporation of the 3HV monomer in the copolymer at a content of 23 ± 4 mol% was observed. A regular random copolymer with a high molecular weight of approximately 1000 kDa and a remarkably low polydispersity index of approximately 1.5 was produced. This feeding strategy maximizes both the productivity and conversion yield of propionic acid into the P(3HB-co-3HV) copolymer if operated close to the critical threshold in the specific rate (q_{PAcrit}).

0.78 $g.L^{-1}.h^{-1}$ and 0.59 $Cmol.Cmol^{-1}$ were reached in this work, which are the best values reported for *C. necator* with propionic acid as the sole substrate. At the industrial scale, it could be implemented as an easy-to-handle and very efficient bioprocess.

In addition, for the first time, with the work performed with sequential feeding in C-overflow conditions (i.e., above the critical specific feeding rate), the residual concentration of propionic acid has been highlighted as a key parameter in 3HV content improvement. In addition, the molecular weight and polydispersity index were not impacted. On the other hand, the yield and productivity that could be reached in C-limiting conditions was reduced. Depending on production goals and constraints, compromises must be made. Nevertheless, the link between feeding strategy (C-overflow vs. C-limitation) and comonomer compositional distribution is not fully understood to date. Additional studies should be performed to assess whether the control of the residual PA concentration could control the 3HV content.

Data availaibility

All data of figures and some additional research data are available in the following repository https://entrepot.recherche.data.gouv.fr/dataverse/loop4pack at https://doi.org/10.57745/OTINNQ .

Acknowledgement

The authors are very grateful to Claudine Charpentier and Véronique Perrier for technical assistance, Véronique Martinez for everyday-life troubleshooting at the biotech lab, Eric Dubreucq, Laurent Rouméas and Robin Boiron for chemical lab equipment resources and Alexis Bessière for polymer extraction and DSC measurements. The authors also thank Jérome Lecomte for scientific discussion on chemical extraction of polymers, Philippe Dieudonné-George for WAXS analysis, Cédric Totee for NMR measurements, Stéphanie Dupoiron and Quentin Subrenat-Margariti for SEC analysis and the Carnot 3BCar institute (consolidation project CARAPOLSEC) who supported the SEC-MALS method development. We finally thank Etienne Paul, Elise Blanchet, Mattéo Castiello and Fanny Allayaud for scientific discussions in the frame of the LOOP4PACK project.

Funding

This work was performed in the framework of the LOOP4PACK project https://projet-loop4pack.fr/en/welcome/ , which is supported by the French National Research Agency (ANR) [Grant Agreement N#ANR-19-CE43-0006].

CRediT authorship contribution statement

Coline Perdrier: Conceptualization, Investigation, Formal analysis, Writing - original draft, Writing - review & editing, Visualization. **Estelle Doineau**: Conceptualization, Investigation, Formal analysis, Writing - original draft, Writing - review & editing. **Ludivine Leroyer:** Methodology, Investigation. **Maeva Subileau:** Writing - review & editing, Resources**. Hélène Angellier-Coussy:** Conceptualization, Formal analysis, Supervision, Project administration, Writing - review & editing, Funding acquisition, Resources. **Laurence Preziosi-Belloy:** Conceptualization, Methodology, Investigation, Formal analysis, Supervision, Writing - review & editing, Project administration, Resources. **Estelle Grousseau:** Conceptualization, Methodology, Investigation, Formal analysis, Supervision, Writing - review & editing, Project administration, Funding acquisition, Resources.

Appendix A. Supplementary Material

Supplementary material of this work can be found in the online version of the paper and consists of S1: Details of broth volume calculation, S2: Details of theoretical RQ calculation and results, S3: Theoretical yields, and S4: Maintenance energy calculation with the Herbert-Pirt equation

Research Data

Supplementary data associated with this article can be found in the online version at https://doi.org/10.1016/j.procbio.2023.02.006

Declaration of interest

None

References

[1] M. Kumar, R. Rathour, R. Singh, Y. Sun, A. Pandey, E. Gnansounou, K.Y. Andrew Lin, D.C.W. Tsang, I.S. Thakur, Bacterial polyhydroxyalkanoates: Opportunities, challenges, and prospects, J. Clean. Prod. 263 (2020) 121500. https://doi.org/10.1016/j.jclepro.2020.121500.

[2] A. Ferre-Guell, J. Winterburn, Biosynthesis and characterization of polyhydroxyalkanoates with controlled composition and microstructure, Biomacromolecules. 19 (2018) 996–1005. https://doi.org/10.1021/acs.biomac.7b01788.

[3] M. V Arcos-hernández, B. Laycock, B.C. Donose, S. Pratt, P. Halley, S. Al-Luaibi, A. Werker, P.A. Lant, Physicochemical and mechanical properties of mixed culture polyhydroxyalkanoate (PHBV), Eur. Polym. J. 49 (2013) 904–913. https://doi.org/10.1016/j.eurpolymj.2012.10.025.

[4] Y. Wang, S. Yamada, N. Asakawa, T. Yamane, N. Yoshie, Y. Inoue, Comonomer compositional distribution and thermal and morphological characteristics of bacterial poly(3-hydroxybutyrate-co-3-hydroxyvalerate)s with high 3-hydroxyvalerate content, Biomacromolecules. 2 (2001) 1315–1323. https://doi.org/10.1021/bm010128o.

[5] Y.J. Sohn, J. Son, S.Y. Jo, S.Y. Park, J.I. Yoo, K.-A. Baritugo, J.G. Na, J. Choi, H.T. Kim, J.C. Joo, S.J. Park, Chemoautotroph *Cupriavidus necator* as a potential game-changer for global warming and plastic waste problem: A review, Bioresour. Technol. 340 (2021) 125693. https://doi.org/10.1016/j.biortech.2021.125693.

[6] G.M.F. Aragao, N.D. Lindley, J.L. Uribelarrea, A. Pareilleux, Maintaining a controlled residual growth capacity increases the production of PHA copolymers by *Alcaligenes eutrophus*, Biotechnol. Lett. 18 (1996) 937–942. https://doi.org/10.1007/BF00154625.

[7] G. Lefebvre, M. Rocher, G. Braunegg, Effect of low dissolved-oxygen concentrations on (3-hydroxybutyrate-co-3-Hydroxyvalerate) production by *Alcaligenes eutrophus*, Appl. Environ. Microbiol. 63 (1997) 827–833. https://doi.org/10.1128/aem.63.3.827-833.1997.

[8] H.W. Ryu, K.S. Cho, B.S. Kim, Y.K. Chang, H.N. Chang, H.J. Shim, Mass production of poly(3-hydroxybutyrate) by fed-batch cultures of *Ralstonia eutropha* with nitrogen and phosphate limitation, J. Microbiol. Biotechnol. 9 (1999) 751–756.

[9] S.Y. Lee, H.H. Wong, J. Choi, S.H. Lee, S.C. Lee, C.S. Han, Production of medium-chain-length polyhydroxyalkanoates by high-cell-density cultivation of *Pseudomonas putida* under

phosphorus limitation, Biotechnol. Bioeng. 68 (2000) 466–470. https://doi.org/10.1002/(SICI)1097-0290(20000520)68:4<466::AID-BIT12>3.0.CO;2-T.

[10] J. Możejko-Ciesielska, T. Pokoj, Exploring nutrient limitation for polyhydroxyalkanoates synthesis by newly isolated strains of *Aeromonas* sp. using biodiesel-derived glycerol as a substrate, PeerJ. 2018 (2018). https://doi.org/10.7717/peerj.5838.

[11] E. Grousseau, E. Blanchet, S. Déléris, M.G.E. Albuquerque, E. Paul, J.L. Uribelarrea, Phosphorus limitation strategy to increase propionic acid flux towards 3-hydroxyvaleric acid monomers in *Cupriavidus necator*, Bioresour. Technol. 153 (2014) 206–215. https://doi.org/https://doi.org/10.1016/j.biortech.2013.11.072.

[12] S. Bellini, T. Tommasi, D. Fino, Poly(3-hydroxybutyrate) biosynthesis by *Cupriavidus necator*: A review on waste substrates utilization for a circular economy approach, Bioresour. Technol. Reports. 17 (2022) 100985. https://doi.org/10.1016/j.biteb.2022.100985.

[13] Y. Doi, A. Tamaki, M. Kunioka, K. Soga, Production of copolyesters of 3-Hydroxybutyrate and 3-Hydroxyvalerate by *Alcaligenes eutrophus* from butyric and pentanoic acids, Appl. Microbiol. Biotechnol. 28 (1988) 330–334. https://doi.org/10.1007/BF00268190.

[14] G. Du, Y. Si, J. Yu, Inhibitory effect of medium-chain-length fatty acids on synthesis of polyhydroxyalkanoates from volatile fatty acids by *Ralstonia eutropha*, Biotechnol. Lett. 23 (2001) 1613–1617. https://doi.org/10.1023/A:1011916131544.

[15] G.C. Du, J. Chen, J. Yu, S. Lun, Feeding strategy of propionic acid for production of poly(3-hydroxybutyrate-co-3-hydroxyvalerate) with *Ralstonia eutropha*, Biochem. Eng. J. 8 (2001) 103–110. https://doi.org/10.1016/S1369-703X(01)00091-2.

[16] B.S. Kim, S.C. Lee, S.Y. Lee, H.N. Chang, Y.K. Chang, S.I. Woo, Production of poly(3-hydroxybutyric-co-3-hydroxyvaleric acid) by fed-batch culture of *Alcaligenes eutrophus* with substrate control using on-line glucose analyzer, Enzyme Microb. Technol. 16 (1994) 556–561. https://doi.org/10.1016/0141-0229(94)90118-X.

[17] A.S. Kelley, D.E. Jackson, C. Macosko, F. Srienc, Engineering the composition of co-polyesters synthesized by *Alcaligenes eutrophus*, Polym. Degrad. Stab. 59 (1998) 187–190. https://doi.org/10.1016/s0141-3910(97)00177-8.

[18] M. Zinn, H.U. Weilenmann, R. Hany, M. Schmid, T. Egli, Tailored synthesis of poly([R]-3-hydroxybutyrate-co-3-hydroxyvalerate) (PHB/HV) in *Ralstonia eutropha* DSM 428, Acta Biotechnol. 23 (2003) 309–316. https://doi.org/https://doi.org/10.1002/abio.200390039.

[19] L.S. Serafim, P.C. Lemos, M.G.E. Albuquerque, M.A.M. Reis, Strategies for PHA production by mixed cultures and renewable waste materials, Appl. Microbiol. Biotechnol. 81 (2008) 615–628. https://doi.org/10.1007/s00253-008-1757-y.

[20] K. Szacherska, P. Oleskowicz-Popiel, S. Ciesielski, J. Mozejko-Ciesielska, Volatile fatty acids as carbon sources for polyhydroxyalkanoates production, Polymers (Basel). 13 (2021) 1–21. https://doi.org/10.3390/polym13030321.

[21] G. Croxatto Vega, J. Voogt, J. Sohn, M. Birkved, S.I. Olsen, G.C. Vega, J. Voogt, J. Sohn, M. Birkved, S.I. Olsen, Assessing new biotechnologies by combining TEA and TM-LCA for an efficient use of biomass resources, Sustain. 12 (2020) 3676. https://doi.org/10.3390/su12093676.

[22] M. Nieder-Heitmann, K.F. Haigh, J.F. Görgens, Life cycle assessment and multi-criteria analysis of sugarcane biorefinery scenarios: Finding a sustainable solution for the South African sugar industry, J. Clean. Prod. 239 (2019) 118039. https://doi.org/10.1016/j.jclepro.2019.118039.

[23] A. Roibás-Rozas, A. Mosquera-Corral, A. Hospido, Environmental assessment of complex wastewater valorisation by polyhydroxyalkanoates production, Sci. Total Environ. 744 (2020) 140893. https://doi.org/10.1016/j.scitotenv.2020.140893.

[24] P. Kumar, S. Ray, V.C. Kalia, Production of co-polymers of polyhydroxyalkanoates by regulating the hydrolysis of biowastes, Bioresour. Technol. 200 (2016) 413–419. https://doi.org/10.1016/j.biortech.2015.10.045.

[25] C. Vidal-Antich, N. Perez-Esteban, S. Astals, M. Peces, J. Mata-Alvarez, J. Dosta, Assessing the potential of waste activated sludge and food waste co-fermentation for carboxylic acids production, Sci. Total Environ. 757 (2021) 143763. https://doi.org/10.1016/j.scitotenv.2020.143763.

[26] M.G.E. Albuquerque, M. Eiroa, C. Torres, B.R. Nunes, M.A.M. Reis, Strategies for the development of a side stream process for polyhydroxyalkanoate (PHA) production from sugar cane molasses, J. Biotechnol. 130 (2007) 411–421. https://doi.org/10.1016/j.jbiotec.2007.05.011.

[27] G. Du, L.X.L. Chen, J. Yu, High-efficiency production of bioplastics from biodegradable organic solids, J. Polym. Environ. 12 (2004) 89–94. https://doi.org/10.1023/B:JOOE.0000010054.58019.21.

[28] J. Yu, Production of PHA from starchy wastewater via organic acids, J. Biotechnol. 86 (2001) 105–112. https://doi.org/10.1016/s0168-1656(00)00405-3.

[29] A.R. Gouveia, E.B. Freitas, C.F. Galinha, G. Carvalho, A.F. Duque, M.A.M. Reis, Dynamic change of pH in acidogenic fermentation of cheese whey towards polyhydroxyalkanoates production: impact on performance and microbial population, N. Biotechnol. 37 (2017) 108–116. https://doi.org/10.1016/j.nbt.2016.07.001.

[30] G. Moretto, F. Valentino, P. Pavan, M. Majone, D. Bolzonella, Optimization of urban waste fermentation for volatile fatty acids production, Waste Manag. 92 (2019) 21–29. https://doi.org/10.1016/j.wasman.2019.05.010.

[31] C. Marangoni, A. Furigo, G.M. Falcão De Aragão, Oleic acid improves poly(3-hydroxybutyrate-co-3-hydroxyvalerate) production by *Ralstonia eutropha* in inverted sugar and propionic acid, Biotechnol. Lett. 22 (2000) 1635–1638. https://doi.org/10.1023/A:1005684525264.

[32] G. Gahlawat, S.K. Soni, Valorization of waste glycerol for the production of poly (3-hydroxybutyrate) and poly (3-hydroxybutyrate-co-3-hydroxyvalerate) copolymer by *Cupriavidus necator* and extraction in a sustainable manner, Bioresour. Technol. 243 (2017) 492–501. https://doi.org/10.1016/j.biortech.2017.06.139.

[33] M.G.E. Albuquerque, V. Martino, E. Pollet, L. Avérous, M.A.M. Reis, Mixed culture polyhydroxyalkanoate (PHA) production from volatile fatty acid (VFA)-rich streams: Effect of substrate composition and feeding regime on PHA productivity, composition and properties, J. Biotechnol. 151 (2011) 66–76. https://doi.org/10.1016/j.jbiotec.2010.10.070.

[34] L.A. Madden, A.J. Anderson, J. Asrar, Synthesis and characterization of poly(3-hydroxybutyrate)

and poly(3-hydroxybutyrate-co-3-hydroxyvalerate) polymer mixtures produced in high-density fed-batch cultures of *Ralstonia eutropha* (*Alcaligenes eutrophus*), Macromolecules. 31 (1998) 5660–5667. https://doi.org/10.1021/ma980606w.

[35] Y. Ishihara, H. Shimizu, S. Shioya, Mole fraction control of poly(3-hydroxybutyric-co-3-hydroxyvaleric) acid in fed-batch culture of *Alcaligenes eutrophus*, J. Ferment. Bioeng. 81 (1996) 422–428. https://doi.org/10.1016/0922-338X(96)85143-9.

[36] J.H. Yun, S.S. Sawant, B.S. Kim, Production of polyhydroxyalkanoates by Ralstonia eutropha from volatile fatty acids, Korean J. Chem. Eng. 30 (2013) 2223–2227. https://doi.org/10.1007/s11814-013-0190-9.

[37] G. Kobayashi, K. Tanaka, H. Itoh, T. Tsuge, K. Sonomoto, A. Ishizaki, Fermentative production of P(3HB-co-3HV) from propionic acid by *Alcaligenes eutrophus* in fed-batch culture with pH-stat continuous substrate feeding method, Biotechnol. Lett. 22 (2000) 1067–1069. https://doi.org/10.1023/A:1005650132371.

[38] J.H. Kim, B.G. Kim, C.Y. Choi, Effect of propionic acid on Poly(Beta-Hydroxybutyric-Co-Beta-Hydroxyvaleric) acid production by *Alcaligenes eutrophus*, Biotechnol. Lett. 14 (1992) 903–906. https://doi.org/10.1007/BF01020626.

[39] F. Huschner, E. Grousseau, C.J. Brigham, J. Plassmeier, M. Popovic, C. Rha, A.J. Sinskey, Development of a feeding strategy for high cell and PHA density fed-batch fermentation of *Ralstonia eutropha* H16 from organic acids and their salts, Process Biochem. 50 (2015) 165–172. https://doi.org/10.1016/j.procbio.2014.12.004.

[40] L. Belfares, M. Perrier, B.A. Ramsay, J.A. Ramsay, M. Jolicoeur, C. Chavarie, Multi-inhibition kinetic model for the growth of *Alcaligenes eutrophus*, Can. J. Microbiol. 41 (1995) 249–256. https://doi.org/10.1139/m95-193.

[41] M.S.I. Mozumder, H. De Wever, E.I.P. Volcke, L. Garcia-Gonzalez, A robust fed-batch feeding strategy independent of the carbon source for optimal polyhydroxybutyrate production, Process Biochem. 49 (2014) 365–373. https://doi.org/10.1016/j.procbio.2013.12.004.

[42] E. Grousseau, E. Blanchet, S. Déléris, M.G.E. Albuquerque, E. Paul, J.-L. Uribelarrea, Impact of sustaining a controlled residual growth on polyhydroxybutyrate yield and production kinetics in *Cupriavidus necator*, Bioresour. Technol. 148 (2013) 30–38. https://doi.org/10.1016/j.biortech.2013.08.120.

[43] A. Werker, P. Lind, S. Bengtsson, F. Nordström, Chlorinated-solvent-free gas chromatographic analysis of biomass containing polyhydroxyalkanoates, Water Res. 42 (2008) 2517–2526. https://doi.org/10.1016/j.watres.2008.02.011.

[44] S. Jan, C. Roblot, G. Goethals, J. Courtois, B. Courtois, J.E.N.E.N. Saucedo, J.P.P. Seguin, J.N.N. Barbotin, Study of parameters affecting poly(3-Hydroxybutyrate) Quantification by Gas Chromatography, Anal. Biochem. 225 (1995) 258–263. https://doi.org/10.1006/abio.1995.1151.

[45] W. Borzani, Calculation of fermentation parameters from the results of a batch test taking account of the volume of biomass in the fermenting medium, Biotechnol. Lett. 25 (2003) 1953–1956. https://doi.org/10.1023/B:BILE.0000003993.76731.9c.

[46] W. Borzani, Calculation of fermentation parameters from the results of a fed-batch test taking

account of the volume of biomass in the fermenting medium, Brazilian Arch. Biol. Technol. 51 (2008) 441–446. https://doi.org/10.1590/S1516-89132008000300001.

[47] S.J. Pirt, The Maintenance Energy of Bacteria in Growing Cultures, Proc. R. Soc. B Biol. Sci. 163 (1965) 224–231. https://doi.org/10.1098/rspb.1965.0069.

[48] A. Burniol-Figols, C. Varrone, A.E. Daugaard, S.B. Le, I. V Skiadas, H.N. Gavala, Polyhydroxyalkanoates (PHA) production from fermented crude glycerol: study on the conversion of 1,3-propanediol to PHA in mixed microbial consortia, Water Res. 128 (2018) 255–266. https://doi.org/10.1016/j.watres.2017.10.046.

[49] M. V Cruz, D. Araújo, V.D. Alves, F. Freitas, M.A.M. Reis, Characterization of medium chain length polyhydroxyalkanoate produced from olive oil deodorizer distillate, Int. J. Biol. Macromol. 82 (2016) 243–248. https://doi.org/10.1016/j.ijbiomac.2015.10.043.

[50] A. Bello, G.M. Guzman, Specific refractive index increments of polymers and copolymers in several solvents, Eur. Polym. J. 2 (1966) 85–91. https://doi.org/https://doi.org/10.1016/0014-3057(66)90063-2.

[51] A. Kovalcik, L. Sangroniz, M. Kalina, K. Skopalova, P. Humpolíček, M. Omastova, N. Mundigler, A.J. Müller, Properties of scaffolds prepared by fused deposition modeling of poly(hydroxyalkanoates), Int. J. Biol. Macromol. 161 (2020) 364–376. https://doi.org/10.1016/j.ijbiomac.2020.06.022.

[52] J. Bossu, H. Angellier-Coussy, C. Totee, M. Matos, M. Reis, V. Guillard, Effect of the molecular structure of poly(3-hydroxybutyrate-co-3-hydroxyvalerate) (P(3HB-3HV)) produced from mixed bacterial cultures on its crystallization and mechanical properties, Biomacromolecules. 21 (2020) 4709–4723. https://doi.org/10.1021/acs.biomac.0c00826.

[53] N. Kamiya, Y. Yamamoto, Y. Inoue, R. Chujo, Y. Doi, Microstructure of bacterially synthesized poly(3-hydroxybutyrate-co-3-hydroxyvalerate), Macromolecules. 22 (1989) 1676–1682. https://doi.org/10.1021/ma00194a030.

[54] N. Yoshie, H. Menju, H. Sato, Y. Inoue, Complex composition distribution of poly(3-hydroxybutyrate-co-3-hydroxyvalerate), Macromolecules. 28 (1995) 6516–6521. https://doi.org/10.1021/ma00123a018.

[55] G. Braunegg, G. Lefebvre, G. Renner, A. Zeiser, G. Haage, K. Loidllanthaler, Kinetics as a tool for polyhydroxyalkanoate production optimization, Can. J. Microbiol. 41 (1995) 239–248.

[56] L. Cavaillé, Production de poly-hydroxy-butyrates à partir d'acides gras volatils en culture ouverte : Influence du degré de limitation en phosphore sur les réponses cinétiques et les sélections microbiennes, Université de Toulouse, Institut National des Sciences Appliquées de Toulouse, 2015.

[57] B. Laycock, P. Halley, S. Pratt, A. Werker, P. Lant, The chemomechanical properties of microbial polyhydroxyalkanoates, Prog. Polym. Sci. 39 (2014) 397–442. https://doi.org/10.1016/j.progpolymsci.2013.06.008.

[58] E. Grousseau, Potentialités de production de Poly-Hydroxy-Alcanoates chez *Cupriavidus necator* sur substrats de type acides gras volatils : études cinétiques et métaboliques., Université de Toulouse, Institut National des Sciences Appliquées de Toulouse, 2012.

[59] Y.J. Chung, H.J. Cha, J.S. Yeo, Y.J.E. Yoo, Production of poly(3-hydroxybutyric-co-3-

hydroxyvaleric)acid using propionic acid by pH regulation, J. Ferment. Bioeng. 83 (1997) 492–495. https://doi.org/10.1016/S0922-338X(97)83009-7.